Table S1: Crystallization conditions, data collection and refinement statistics.
* : the number in parenthesis indicates the probable oligomeric assembly. ** : only the ADP moiety of ATPγS is visible in the refined structure.

	EfFIC^{WT}- PO_4^{2-}	**EfFIC^{WT}**	**EfFIC^{WT}-AMP-Ca^{2+}**
PDB accession code	6ER8	5NV5	6EP0
Data collection			
Space group	$P4_12_12$	I222	$P4_12_12$
Molecules in a.u.*	2 (2)	4 (2)	2 (2)
a, *b*, *c* (Å)	65.13, 65.13, 248.06	121.54, 131.00, 136.94	64.98 64.98 246.24
α, β, γ (°)	90.00, 90.00, 90.00	90.00, 90.00, 90.00	90.00, 90.00, 90.00
Resolution (Å)	44.91-2.29 (2.38-2.29)	47.33-2.40 (2.49-2.40)	82.08-2.35 (2.48-2.35)
R_{merge}	0.312 (1.808)	0.087 (0.665)	0.139 (1.146)
I / σI	5.2 (1.4)	13.5 (2.2)	13.1 (2.3)
Completeness (%)	94.8 (91.7)	99.8 (97.6)	100.0 (100.0)
Multiplicity	4 (2.8)	5.6 (5.4)	16.7 (17.8)
Concentration	10mg/mL	13mg/mL	8mg/mL
Buffer	50mM Tris pH 8.0 100mM NaCl 1mM $MgCl_2$ 1mM DTT 10mM NAD	50mM Tris pH 8.0 100mM NaCl 10mM ADP	50mM Tris pH 8.0 100mM NaCl 5mM AMP
Precipitant	0.16M Calcium acetate 0.08M Sodium cacodylate pH 6.5 14.4% (w/v) PEG 8000 20% (v/v) Glycerol	50mM Bicine pH 8.4 30% (w/v) PEG 2000 MME	0.2M Calcium Chloride 0.1M HEPES sodium salt pH 7.5 28% (v/v) PEG 400
Cryoprotectant	none	none	none
Beamline	Proxima1	ID30A-3	ID29
Data processing	xdsme	xdsme	autoproc
MR model	NmFIC 2G03	6ER8	6ER8
Ligand	PO_4^{2-}	-	AMP-Ca^{2+}
Refinement			
Resolution (Å)	2.29	2.40	2.35
No. reflections	23571	42957	22951
R_{work} / R_{free}	0.229/0.298	0.164/0.226	0.2018/0.264
No. atoms	3653	7316	3530
B-factors	35.47	44.03	61.1
R.m.s. deviations			
Bond lengths (Å)	0.008	0.010	0.010
Bond angles (°)	0.893	1.08	1.08

Table S1, continued

	EfFIC^{WT}-ATPγS-Ca^{2+}	**EfFIC^{WT}- ATPγS**
PDB accession code	6EP2	6EP5
Data collection		
Space group	$P4_32_12$	$P4_32_12$
Molecules in a.u.*	12 (6)	6 (6)
a, *b*, *c* (Å)	125.35 125.35 362.8	87.84 87.84 364.94
α, β, γ (°)	90.00 90.00 90.00	90.00 90.00 90.00
Resolution (Å)	118.45-2.15 (2.19-2.15)	47.3-1.93 (1.96-1.93)
R_{merge}	0.21 (1.952)	0.172 (2.806)
I / σI	10.5 (2.1)	9.8 (0.8)
Completeness (%)	100 (100)	99.9 (97.3)
Multiplicity	16.9 (17.7)	13.0 (12.6)
Concentration	8mg/mL	13mg/mL
Buffer	20 mM Hepes pH 7.4 200mM NaCl 5mM MgCl2 5mM ATPγS	50mM Tris pH 8.0 100mM NaCl 5mM ATPγS
Precipitant	14.4 % w/v PEG 8,000 20 % v/v glycerol 80 mM MES; pH 6.5 160 mM Calcium acetate	2M Ammonium sulfate 0.1M Bis-Tris pH 5.5
Cryoprotectant	none	none
Beamline	Proxima1	ID30B
Data processing	xdsme	xdsme
MR model	6ER8	6ER8
Ligand	ATPγS–Ca^{2+}**	ATPγS **
Refinement		
Resolution (Å)	2.15	1.93
No. reflections	157231	108653
R_{work} / R_{free}	0.1869/0.2178	0.2003/0.2402
No. atoms	22152	11142
B-factors	41.95	33.71
R.m.s. deviations		
Bond lengths (Å)	0.005	0.007
Bond angles (°)	0.947	0.992

Table S1, continued

	EfFIC^{H111A}	**EfFIC^{H111A} -SO_4^{2-}**
PDB accession code	5NWF	6ERB
Data collection		
Space group	$P2_122_1$	I222
Molecules in a.u. *	2 (4)	4 (2)
a, b, c (Å)	76.67 77.11 103.15	121.93 131.16 136.71
α, β, γ (°)	90.00, 90.00, 90.00	90.00, 90.00, 90.00
Resolution (Å)	103.15-2.60 (2.72-2.60)	47.32-2.20 (2.26-2.20)
R_{merge}	0.072 (0.499)	0.081 (1.321)
I / σI	15.5 (3.6)	18.5 (2.1)
Completeness (%)	99.1 (99.9)	100.0 (100.0)
Multiplicity	5.9 (6.1)	13.7 (14.2)
Concentration	10mg/mL	7mg/mL
Buffer	50mM Tris pH 8.0 200mM NaCl 1mM MgCl2	50mM Tris pH 8.0 150mM NaCl 2mM ATPγS 2mM MgCl2
Precipitant	0.2M Ammonium sulfate 0.1M Tris-sodium citrate pH 5.6 15% (w:v) PEG 4000	0.2M Lithium Sulfate 0.1M Tris pH 8.5 20% (w/v) PEG 4000
Cryoprotectant	none	none
Beamline	Proxima2a	Proxima2a
Data processing	xdsme	xdsme
MR model	6ER8	6ER8
Ligand	-	SO_4^{2-}
Refinement		
Resolution (Å)	2.6	2.2
No. reflections	19240	55796
R_{work} / R_{free}	0.191/0.250	0.2132/0.2488
No. atoms	3516	7095
B-factors	62.79	54.64
R.m.s. deviations		
Bond lengths (Å)	0.008	0.008
Bond angles (°)	1.103	1.012

Veyron et al. Supplementary data.

Analysis of the deAMPylation catalytic mechanism of EfFIC.

We discuss below the mechanism of deAMPylation of EfFIC. First, it should be noted that FIC active sites do not ressemble the active site of Legionella de-AMPylase SidD, which has a canonical phosphatase fold (1) or the de-AMPylation domain of E. coli glutamine synthase adenylyl transferase (2), hence are not expected to share catalytic features with these enzymes. From a general enzymology perspective, two major mechanisms of (phospho)ester bond hydrolysis can be considered: anchimeric catalysis, which is assisted by the substrate (**Figure S2A)** or conventional acido-basic catalysis **(Figure S2B**). Both mechanisms involve four steps (see **Figure S2**) and share three chemical requirements: i) a proton attractor to increase the nucleophilic properties of the reactive oxygen (step 1) ii) a positively charged species, located in the neighborhood of the phosphate group to increase the susceptibility of the phosphorus to nucleophilic attack and stabilize the developing negative charge in the intermediate (steps 2 and 3), and iii) a proton donor, located close to the cleaved phosphor-ester bond to favor the production of the leaving group by giving up its proton (step 4). A major difference between the two scenarii is that nucleophilic attack is performed by the 2' hydroxyl of the ribose in the anchimeric mechanism, as described for a calcium-dependent phosphoinositide-specific phospholipase C from Pseudomonas (3), whereas it is achieved by the oxygen of an activated water molecule in the general acido-basic catalysis. The two mechanisms can be distinguished by at least two major features of the active site: i) anchimeric catalysis requires a proton attractor close to the ribose 2'OH, whereas the general acidic catalysis requires a proton attractor close to the nucleophilic water molecule, itself located close to the leaving phosphate group; ii) substrate-activated catalysis involves the formation of a cycle between the phosphorus and the 2'OH of the AMP moiety of the substrate.

Considering our EfFIC^{WT}-AMP-Ca^{2+} structure as an acceptable mimic of the enzyme-AMPylated protein complex, EfFIC displays several important features: i) the AMP moiety is stabilized by multiple interactions with the active site, such that a large conformational change needed for cyclisation in the anchimeric reaction is unlikely ii) a water molecule coordinated by the conserved glutamate and Ca^{2+} ion can be readily positionned for in line nucleophilic attack by completing the heptahedral coordination of Ca^{2+} iii) no proton acceptor is situated closed to the 2'OH in the structures. Together, these observations impose a

mechanism based on acido-basic and electrostatic catalysis, as described in **Figures 5** and **S2B**.

Supplementary Figure legends

Figure S1 (associated with Figures 1 and 2). Structural analysis of EfFIC.

1A: Omit map showing the electron density of the inhibitory glutamate and the ADP moiety of ATPγS in $EfFIC^{WT}$-ATPγS contoured at 5.0 r.m.s.d.. The electron density of Glu190 is representative of all EfFIC structures determined in this study

1B: Omit map showing the electron density of Ca^{2+} in $EfFIC^{WT}$-AMP-Ca^{2+}-bound structure contoured at 10.0 r.m.s.d.

Figure S2 (associated with Figure 5). Comparison of anchimeric and acido-basic deAMPylation catalytic mechanisms.

2A: Anchimeric catalysis.

2B: Acido-basic catalysis.

Both mechanisms involve four steps, as indicated: (1) activation of the reactive oxygen through proton attraction (2); nucleophilic attack on the positively charged phosphorus triggering P=O π electrons rearrangement and production of a pentavalent intermediate harboring an additional negative charge; (3) stabilization of the intermediate by a positive charge in the catalytic site, which also contribute to elicit the electrophily of the phosphorus and (4) facilitation of phosphor-ester bond cleavage through protonation of the leaving hydroxylate group. R: AMPylated protein. A- : basic form of an acidic catalyst (proton attractor). BH+ : acidic form of a basic catalyst (proton donor).

References

1. Chen Y*, et al.* (2013) Structural basis for Rab1 de-AMPylation by the Legionella pneumophila effector SidD. *PLoS pathogens* 9(5):e1003382.
2. Xu Y, Carr PD, Vasudevan SG, & Ollis DL (2010) Structure of the adenylylation domain of E. coli glutamine synthetase adenylyl transferase: evidence for gene duplication and evolution of a new active site. *J Mol Biol* 396(3):773-784.
3. Moroz OV*, et al.* (2017) The structure of a calcium-dependent phosphoinositide-specific phospholipase C from Pseudomonas sp. 62186, the first from a Gram-negative bacterium. *Acta Crystallogr D Struct Biol* 73(Pt 1):32-44.

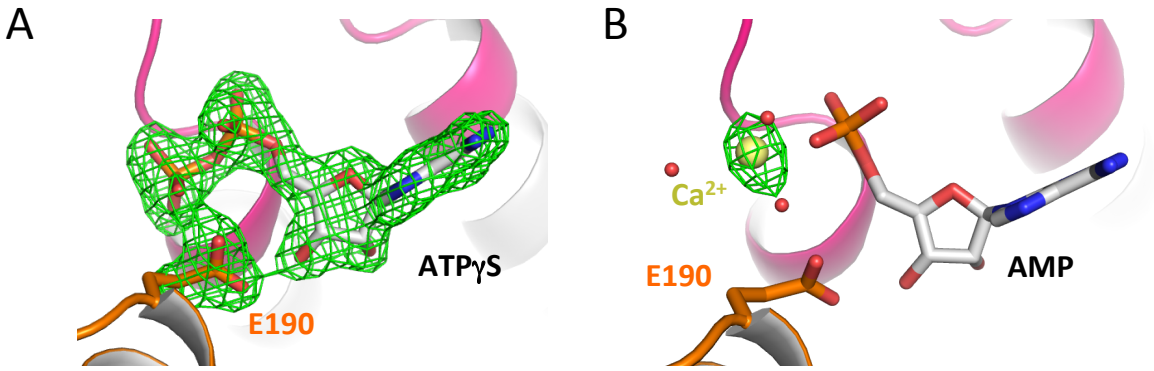

Supplementary Figure S1

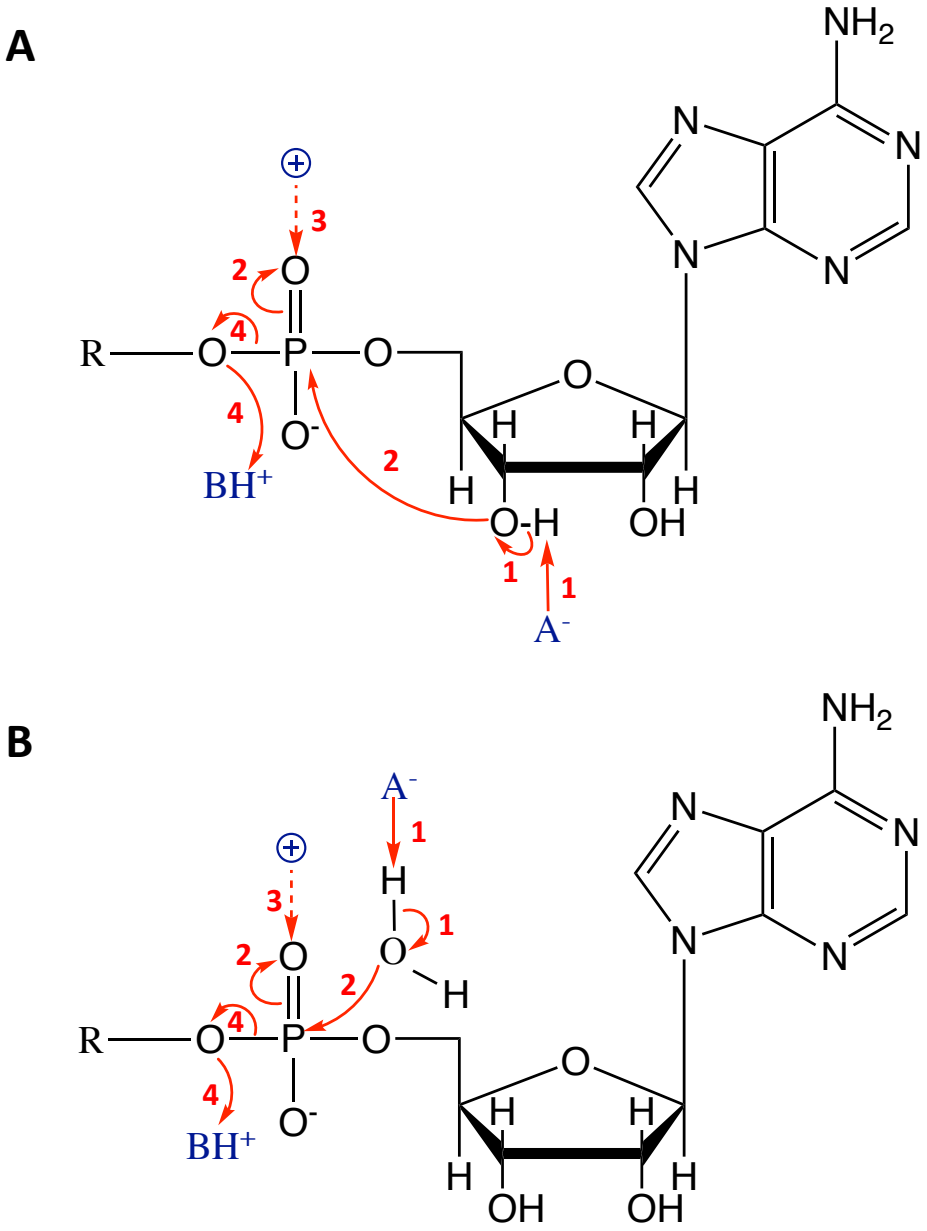

Supplementary Figure S2